



Comparison of water-soluble and water-insoluble organic compositions attributing to different light absorption efficiency between residential coal and biomass burning emissions

Lu Zhang^{1,2}, Jin Li¹, Yaojie Li¹, Xinlei Liu¹, Zhihan Luo¹, Guofeng Shen¹, and Shu Tao^{1,3}

¹Laboratory for Earth Surface Process, College of Urban and Environmental Sciences, Peking University, Beijing 100871, China

²Department of Civil and Environmental Engineering, Hong Kong Polytechnic University, Kowloon, Hong Kong SAR, China

³College of Environmental Science and Technology, Southern University of Science and Technology, Shenzhen 518055, China

Correspondence: Guofeng Shen (gfshen12@pku.edu.cn)

Received: 18 October 2023 – Discussion started: 13 November 2023

Revised: 17 April 2024 – Accepted: 18 April 2024 – Published: 29 May 2024

Abstract. There are growing concerns about the climate impacts of absorbing organic carbon (also known as brown carbon, BrC) in the environment, yet its chemical composition and association with the light absorption capabilities remain poorly understood. This study characterized water-soluble and water-insoluble organic carbon (WSOC and WIOC) from residential solid fuel combustion at the molecular level and evaluated their quantitative relationship with mass absorption efficiency (MAE). The MAE values at $\lambda = 365$ nm from biomass burning were significantly higher than those from coal combustion ($p < 0.05$). Thousands of peaks were identified in the m/z range of 150–800, with the most intense ion peaks occurring between m/z 200–500 for WSOC and m/z 600–800 for WIOC, respectively. The CHO group predominated in the WSOC extract from biomass burning emissions, while sulfur-containing compounds (SOCs) including CHOS and CHONS were more intense in the WIOC extract, particularly from coal emissions. Emissions of the CHON group were positively correlated with the fuel nitrogen content ($r = 0.936$; $p < 0.05$), explaining their higher abundance in coal emissions compared to biomass. The SOC emissions were more predominant during flaming phases, as indicated by a positive correlation with modified combustion efficiency (MCE) ($r = 0.750$; $p < 0.05$). The unique formulas of coal combustion aerosols were in the lower H/C and O/C regions, with higher unsaturated compounds in the van Krevelen (VK) diagram. In the WIOC extract, coal combustion emissions contained significantly higher fractions of condensed aromatics (32%–59%) compared to only 4.3%–9.7% in biomass burning emissions. In contrast, the CHOS group in biomass burning emissions was characterized by larger condensed aromatic compound fractions than those in coal combustion. Moreover, the CHOS aromatic compound fractions were positively correlated with MAE values in both WSOC ($r = 0.714$; $p < 0.05$) and WIOC extracts ($r = 0.929$; $p < 0.001$), suggesting that these compounds significantly contributed to MAE variabilities across different fuels.

1 Introduction

Light-absorbing organic carbon (OC), known as brown carbon (BrC), has attracted growing concern due to its direct radiative impact on climate change (Laskin et al., 2015; Wang et al., 2022). The global simulations suggested that BrC may contribute nearly 20 % of the surface organic aerosol (OA) burden (Jo et al., 2016) and may account for 19 % of the light absorption by anthropogenic aerosols (Feng et al., 2013). BrC originates from diverse sources, including primary emissions from coal combustion, biomass burning, and vehicular emissions (Du et al., 2014; Olson et al., 2015; Bond, 2001; Sun et al., 2017; Chen and Bond, 2010) and secondary processes like the oxidation of volatile organic compounds (Guan et al., 2020; Laskin et al., 2015). Among these sources, residential solid fuel burning produced large amounts of BrC, accounting for 74 % of the total anthropogenic primary emissions (Xiong et al., 2022).

Some efforts have been made to explore the BrC physiochemical properties in residential emissions. For example, water-soluble organic carbon (WSOC) and methanol-soluble organic carbon (MSOC) were analyzed in primary emissions from combustions of crop straw, wood fuel, and some coal (Park and Yu, 2016). Available studies suggested that the optical properties of primary BrC varied significantly and were influenced by numerous factors including inherent fuel properties and combustion conditions. Mass absorption efficiency (MAE) is a key parameter in assessing the direct radiative forcing of light-absorbing carbonaceous aerosols (Huo et al., 2018). It was found that water-soluble BrC derived from bituminous coal had higher MAE values than anthracites (Tang et al., 2020). However, the specific chemical components responsible for the differences in light absorption among various fuel types are not yet fully understood, especially at the molecular level. It was also reported that the mass absorption of water-insoluble organic carbon (WIOC) could be even greater than that of the water-soluble ones (Chen and Bond, 2010; Huang et al., 2018). However, there is limited information available regarding their chemical components. Given the significant variation in BrC light absorption across different fractions emitted from various fuels (Xie et al., 2017), detailed information of a comprehensive characterization, including the chemical and optical characteristics of the BrC fractions (both water-soluble and water-insoluble) from the combustion source, is needed.

This study investigated the chemical compositions and light absorption abilities of WSOC and WIOC in smoke particles generated from the burning of coal with different maturity, raw biomass fuels, and biomass pellets in traditional and improved stoves. The use of biomass pellets has been heavily promoted over the last several years to mitigate air pollutant emissions from traditional solid fuels, and emission characteristics from improved stoves could be different from traditional ones. Optical property variations were quantitatively assessed and analyzed to explore their association

with chemical components. Furthermore, unique molecules and fingerprints for coal and biomass sources were discussed, which is critical in pollution source appointment.

2 Materials and methods

2.1 Laboratory combustion emission experiment

In the present study, a total of 14 types of coal with varying maturity degrees, 5 types of biomass pellets, and 12 types of raw biomass were examined using a laboratory combustion system. Two types of stoves, including a traditional stove (TS) and an improved stove (IS), were utilized for the experiments. The 34 fuel–stove combinations are listed in Table S1 in the Supplement. The combustion tests were performed in a specially designed system with real-time online monitors (Thermo Fisher Scientific Inc., Bremen, Germany) which are capable of continuously measuring gaseous pollutants, including CO, CO₂, hydrocarbons (HCs), and nitrogen oxide (NO_x, including NO and NO₂). PM_{2.5} (particles with aerodynamic diameters ≤ 2.5 μm) was collected at a flow rate of 16.7 L min⁻¹ with quartz filters. Fuel properties including moisture (*M*_{ad}; %); volatile matter content (*V*_{daf}; %); ash content (*A*_{ad}; %); lower heating value (LHV; MJ kg⁻¹); and contents of carbon (C; %), hydrogen (H; %), nitrogen (N; %), and sulfur (S; %) are tested and listed in Table S1. Details of stove construction and combustion processes were available in Zhang et al. (2022).

Modified combustion efficiency (MCE) was calculated by integrating the incremental concentrations of CO₂ and CO as

$$\text{MCE} = \frac{\text{CO}_2}{\text{CO}_2 + \text{CO}},$$

where CO₂ and CO represent the excess molar mixing ratios of CO₂ and CO, respectively (Pokhrel et al., 2016). The MCE values indicate different phases of combustion, i.e., approximately 1 during flaming and between 0.7–0.9 during smoldering (Yokelson et al., 1997)

2.2 Bulk carbon and UV-Vis absorption spectra

For each sample, a 4.9 cm² filter was extracted ultrasonically with 10 mL Milli-Q water (18.2 MΩ) for 30 min, and then the supernatant was separated. The extraction process was repeated twice, and the extracts were combined. The water extract was then filtered via a 0.22 μm polytetrafluoroethylene (PTFE) filter to obtain WSOC. Due to the inefficiency of water in extracting BrC, the insoluble PM components remaining on the sample filter were freeze-dried and subjected to methanol extraction through sonication. The resulting extract was then filtered using a PTFE filter, yielding a water-insoluble fraction referred to as WIOC in the following text. The carbon content of WSOC was analyzed with a total organic carbon (TOC) analyzer (TOC-LCPH/CPN, Shimadzu, Japan), and the WIOC was determined by subtracting WSOC

from the total OC loaded on the same 4.9 cm² area, given that the methanol extraction efficiency for all combustion samples was up to 90 % (Zhang et al., 2022). The elemental carbon (EC) and OC were measured using a thermal–optical analyzer (Sunset OC/EC analyzer) with an interagency monitoring of protected visual environments (IMPROVE) program.

The light absorption spectra of the water and methanol extracts were measured between 200 and 600 nm by an ultraviolet visible (UV-Vis) spectrophotometer (UV-2600, Shimadzu, Japan) at a step size of 1 nm. MAE values of WSOC and WIOC at the wavelength of λ ($\text{MAE}_{\lambda, \text{WSOC}}$; $\text{MAE}_{\lambda, \text{WIOC}}$) were calculated as the following equation (Li et al., 2019):

$$\begin{aligned} \text{MAE}_{\lambda, \text{WSOC}} &= A_{\lambda, \text{WSOC}} \times \ln(10) / (C_{\text{WSOC}} \times L); \text{MAE}_{\lambda, \text{WIOC}} \\ &= A_{\lambda, \text{WIOC}} \times \ln(10) / (C_{\text{WIOC}} \times L), \end{aligned}$$

where $A_{\lambda, \text{WSOC}}$ and $A_{\lambda, \text{WIOC}}$ are the light absorption value of WSOC extract and WIOC extract at a wavelength of λ , respectively. C is the concentration of WSOC (or WIOC), and L is the optical path length, which is 0.01 m in this study. It is important to note that the reported light absorption of WIOC in this study was underestimated; such an underestimation is insignificant due to the high extraction efficiency. In this study, the MAE values of extractable OC at λ of 365 nm ($\text{MAE}_{365, \text{WSOC}}$ and $\text{MAE}_{365, \text{WIOC}}$) were discussed.

Absorption Ångström exponent (AAE) values were determined based on the following equation (Li et al., 2019; Li et al., 2020):

$$A_{\lambda} = K_{\lambda}^{-\text{AAE}},$$

where K is a constant, and AAE is obtained through the linear regression of $\lg(A_{\lambda})$ against $\lg\lambda$ (Fig. S1 in the Supplement). A wavelength of 300–400 nm is chosen according to the published literature (Yue et al., 2022), and the goodness of fit for all the samples in this study is greater than an r^2 of 0.99.

2.3 Molecular composition analysis

For further molecular composition analysis, the WSOC and WIOC extracts from seven selected source samples were subjected to Fourier transform ion cyclotron resonance mass spectrometry (FT-ICR-MS) coupled with electrospray ionization (ESI). These samples included two types of coal (high-volatility bituminous coal, HVB; medium-volatility bituminous coal, MVB) combusted in TS, two types of raw biomass (rice straw and pine wood) combusted in TS, pine wood combusted in IS, and two types of biomass pellets (crop straw pellets and pine wood pellets) combusted in IS, as noted in the Supplement. FT-ICR-MS has been successfully applied for the molecular-level characterization of compounds (Bianco et al., 2018), due to its ultrahigh resolution and mass accuracy. ESI is well adopted to character-

ize soluble aerosols, especially for the detection of polar hydrophilic molecules like humic-like substance (HULIS)-type compounds (Wozniak et al., 2008) because it is a “soft” ionization technique generating minimal analyte fragments and thus can detect intact molecules of compounds. Therefore, the negative ESI-FT-ICR was applied here to determine the molecular compositions of WSOC and WIOC from combustion samples from different solid fuels. The methanol extracts were evaporated to dryness under a gentle stream of nitrogen and then dissolved with Milli-Q water. The WSOC and water-reconstituted WIOC were submitted to solid-phase extraction (SPE) using Bond Elut PPL (500 mg, 6 mL; Agilent, USA). Before extraction, the PPL cartridges were sequentially conditioned with 12 mL methanol and 12 mL Milli-Q water containing 0.05 % hydrochloric acid (HCl). The extract was adjusted to pH = 2 using HCl to remove inorganic ions and was then loaded onto the PPL cartridges at a rate of 5 mL min⁻¹. Cartridges were washed with 18 mL Milli-Q water containing 0.05 % HCl to remove salt and then dried under pure nitrogen. Analytes were eluted with 12 mL methanol, and the combined eluates were concentrated to 1 mL. Then the molecular characterization was conducted using a 15T solariX XR FT-ICR-MS (Bruker Daltonics GmbH & Co. KG, Bremen, Germany) in the negative ESI mode. The capillary inlet voltage was set at -4.0 kV, and the ion accumulation time was set to 0.06 s. There were 300 continuous 4 M data FT-ICR transients added to improve the signal-to-noise ratio. The FT-ICR-MS was calibrated with 10 mmol L⁻¹ sodium formate in advance, and an internal standard calibration with soluble organic matter (known molecular formula) was performed after the test. Finally, < 1 ppm absolute mass error was achieved. Data processing details are described in the Supplement.

3 Result and discussion

3.1 Optical characteristics of WSOC and WIOC

MAE is an important parameter reflecting the light absorption capability of the carbonaceous aerosols. The $\text{MAE}_{365, \text{WSOC}}$ of aerosols from residential sources in this study ranged from 0.21 to 3.1 m² g⁻¹, with an average of 1.3 ± 0.7 m² g⁻¹. MAE values of extractable OC in this study were lower than that of 11.3 m² g⁻¹ for pure BC aerosols (Bond and Bergstrom, 2006) and also lower than that from the filter-based MAE values of OC of 0.16–13 m² g⁻¹ from residential sources (Zhang et al., 2021b). A significant difference ($p < 0.05$) in $\text{MAE}_{365, \text{WSOC}}$ was observed among the different fuels (Fig. 1). The $\text{MAE}_{365, \text{WSOC}}$ of raw biomass-combustion-derived aerosols averaged at 1.7 ± 0.8 m² g⁻¹, which was significantly higher ($p < 0.05$) than those from coal smoke (0.93 ± 0.44 m² g⁻¹) and biomass pellet smoke (1.2 ± 0.6 m² g⁻¹). The $\text{MAE}_{365, \text{WIOC}}$ ranged from 0.49 to 6.6 m² g⁻¹, with an average of 2.0 ± 1.3 m² g⁻¹. The absorption capability was higher for the WIOC extract than

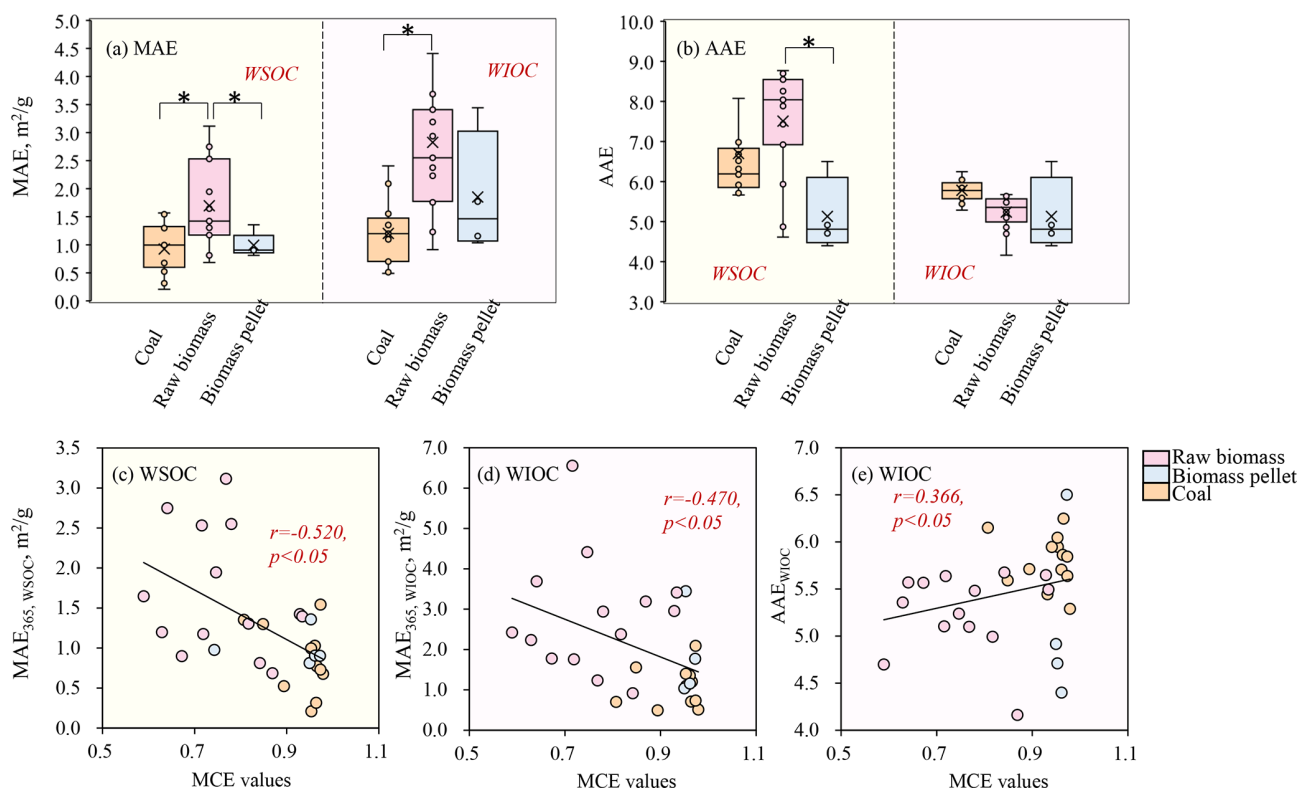


Figure 1. MAE values at $\lambda = 365$ nm (a) and AAE values (b) from the source samples (* represents $p < 0.05$). There is a correlation between the MCE values with MAE_{365,WSOC} values (c), MAE_{365,WIOC} values (d), and AAE_{WIOC} values (e).

the WSOC extract. This is thought to be associated with distinct chemical compositions of light-absorbing organics. It was noted that the WIOC had higher MAE values compared to the WSOC, which may be explained by the more hydrophobic polycyclic aromatic hydrocarbons (PAHs) and quinones (Chen and Bond, 2010). The difference in MAE_{365,WIOC} among the different fuels was also statistically significant ($p < 0.05$), as the value obtained from raw biomass burning ($2.8 \pm 1.4 \text{ m}^2 \text{ g}^{-1}$) was significantly higher than that from coal combustion ($1.2 \pm 0.6 \text{ m}^2 \text{ g}^{-1}$). It was suggested that the MAE values of soluble OC including WSOC and WIOC were dependent on the chemical composition of OC, that is, the chemical structure of the light-absorbing chromophores and the ratio of non-light-absorbing organics to the chromophore components (Cao et al., 2021). The higher MAE values of raw biomass-combustion-derived aerosols might be caused by the stronger light absorption capability of chromophores or a higher ratio of chromophores. Our result was comparable to the published data; for example, the MAE_{365,WSOC} was reported to average at $1.37 \pm 0.23 \text{ m}^2 \text{ g}^{-1}$ for biomass burning emissions (Park and Yu, 2016). The correlation of MAE with the MCE was investigated. The variability in MAE values, for both WSOC and WIOC, was observed to be negatively correlated with the MCE (or temperature, as MCE was found to be posi-

tively correlated with the measured temperature in emission exhausts) when pooling all data together, as seen in Fig. 1c and d. However, within each fuel group, there was no statistically significant correlation between the MAE and MCE values (Fig. S2). Some previous studies found that OC from wood pyrolysis under higher-temperature conditions had a stronger absorption capability (Chen and Bond, 2010; Saleh et al., 2014), but relatively higher mass absorption coefficient (MAC) values were also reported for the organic aerosol from wood combustion under the $150^\circ\text{C} < T < 250^\circ\text{C}$ compared to emissions at a lower- ($T < 150^\circ\text{C}$) or higher-temperature ($250^\circ\text{C} < T < 380^\circ\text{C}$) condition (Rathod et al., 2017). Chen and Bond (2010) reported that absorption per mass (α/ρ) of methanol extracts increased with increased wood pyrolysis temperature, but such an increase was non-linear and varied in burning emissions of different fuel types or wood with different sizes. Therefore, the negative correlations between MAE and MCE values when pooling all data together (in Fig. 1) were from distinct absorption properties of emissions from different fuel types rather than from conditions like combustion temperature.

The AAE which indicates that the wavelength dependence of light absorption is also an important parameter in climate models. The calculated AAE in the WSOC extract (AAE_{WSOC}) ranged from 3.8 to 11, with an average of

6.9 ± 1.5 , and the difference in AAE_{WSOC} values among the different fuels was statistically significant ($p < 0.05$) (Fig. 1). The highest values were observed for the aerosols from raw biomass combustion of 7.5 ± 1.4 , followed by coal smoke of 6.7 ± 1.5 and biomass pellet smoke of 5.6 ± 1.2 . The AAE values in the WIOC extract (AAE_{WIOC}) were slightly lower than AAE_{WSOC} , which ranged from 4.2 to 6.5, with an average of 5.5 ± 0.5 . The differences in AAE_{WIOC} values among the different fuels were statistically insignificant ($p > 0.05$), with averaged values of 5.8 ± 0.3 for coal smoke, 5.1 ± 0.9 for biomass pellet smoke, and 5.2 ± 0.4 for raw biomass smoke. There was a weak positive correlation of AAE_{WIOC} between the MCE values ($p < 0.05$). The filter-based analysis also showed that AAE values were positively correlated with MCE values, indicating that more BrC was produced under the smoldering phase compared with BC (Zhang et al., 2020). This study suggested that BrC in WIOC extract was generated during the smoldering phase in comparison with the non-light-absorbing OC. The AAE values in soluble OC in this study were higher than 4 for all samples, confirming the contribution of BrC to aerosol absorptivity from source emission. The result of this study was comparable to the published literature. For example, it was reported that the AAE_{WSOC} was in the range of 8.6–15 from coal-combustion-derived aerosols (Song et al., 2019) and 6.2–9.3 from biomass smoke (Park and Yu, 2016). The AAE_{WIOC} from wintertime urban aerosols were 5.4 ± 0.2 in Xi'an and 5.7 ± 0.2 in Beijing (Huang et al., 2020).

3.2 Molecular characteristics of WSOC and WIOC

The ESI-FT-ICR-MS of WSOC and WIOC samples are presented in Fig. 2. Thousands of peaks were identified in the m/z range of 150–800, indicating a complex chemical composition of aerosols from residential sources. Formulas detected in the raw biomass burning aerosols were significantly higher than those in biomass pellets and coal smoke (Fig. S3), which indicated a higher chemical complexity of raw biomass emissions. In addition, the combustion of pine wood in the improved stove generated fewer compounds, which was 93 % of the peaks identified in the traditional stove (Table S2). The lower complexity might be due to higher combustion efficiencies and temperature in the improved stove. Generally, higher levels of organic aerosol mass would be emitted during less efficient fuel burning resulting from prolonged smoldering or incomplete burning (Holder et al., 2016). Our results suggested that corresponding higher chemical complexity was also produced during the incomplete combustion in the traditional stove. The most intense ion peaks were distributed in the m/z 200–500 for WSOC, accounting for 58 %–86 % of the total intensity. Similar results were also found in residential coal combustion (Song et al., 2019), biomass burning (Song et al., 2018), and ambient aerosols (Wozniak et al., 2008).

The mass spectra of WIOC are different from the WSOC, especially in aerosol emitted from coal combustion (Fig. 2). WIOC contained more molecules with larger m/z values of 600–800 in the range, which indicated that the WIOC extract had more compounds with a higher molecular weight (MW) than the WSOC extract. According to the molecular formulas and the intensity of each negative ion, the average molecular formulas for the WSOC were obtained with C atom (from 20 to 24), H (21–29), N (0.32–0.75), O (5.6–7.0), and S (0.28–0.51) in the WSOC extract. All aerosols from biomass burning, either raw or pelletized ones, had higher relative O atom contents than coal smoke, indicating a higher oxidation degree of biomass emissions. For the WIOC, the average molecular formulas were assigned with 27–33 C, 26–35 H, 0.67–1.2 N, 6.6–11 O, and 0.34–0.92 S. The coal-combustion-derived aerosols had more C, N, and S atoms but fewer H atoms compared with raw biomass. The combustion of biomass pellets is also assigned with relatively higher S elements. In addition, the WIOC fraction had a higher relative atom content than the corresponding formulas of WSOC from the same source aerosol samples. These results indicated that in addition to the fuel type, the extraction solvent also had an important impact on the elemental composition of extractable BrC.

Molecular formulas identified by the FT-ICR-MS can be classified into four groups according to the elemental composition, including CHO (containing only C, H, O), CHON (similar hereafter), CHOS, and CHONS. CHO was the most abundant group in the WSOC. The CHO group contributed 51 %–67 % to the total intensity of aerosols from raw biomass burning, which was a significantly higher contribution than that of biomass pellets (29 %–39 %) and coal smoke (30 %–40 %). The CHO compounds with oxygen-containing functional groups (e.g., hydroxyl, carbonyl, carboxyl, or esters) have been widely identified in both ambient aerosols (Jiang et al., 2021; Mo et al., 2022) and some source samples (Tang et al., 2020). These compounds contributed a broad range of proportions, with 43 %–69 % from residential biomass burning smoke (Tang et al., 2020), 9.7 %–48 % from coal smoke (Song et al., 2019), and 20 %–39 % from ambient aerosols (He et al., 2023) for the WSOC extract, with values which were comparable to ours. CHON compounds were also an important component in the aerosols, accounting for 29 %–36 % coal smoke, which was significantly higher than the biomass burning smoke of 11 %–28 %. One previous study reported that CHON species were more abundant in biomass burning smoke rather than in coal combustion ones (Song et al., 2018). This high fraction of CHON compounds in coal smoke might be caused by the higher nitrogen content of coal as seen in Table S1. A strongly significantly positive correlation was found between the fuel nitrogen content and CHON species percentage ($r = 0.936$; $p < 0.05$) (Fig. 3). Such dependence was also found in the emission factors (EFs) of NO_x on fuel nitrogen content in our result (Fig. S4), as well as NO_x , HCN, and NH_3 emissions re-



Figure 2. Negative ESI FT-ICR-MS of WSOC (a–g) and WIOC (a1–g1) from the seven aerosol samples. TS represents combustion in the traditional stove, and IS represents combustion in the improved stove. Different formula groups were color-coded. The pie charts showed the relative intensities of different formula groups.

ported by published literature (Hansson et al., 2004). Sulfur-containing compound (SOC; including CHOS and CHONS) abundance was lower than CHO and CHON group, accounting for only 22%–42% (13%–30% for CHOS and 7.9%–28% for CHONS, respectively). The fractions of SOCs in the aerosols from coal combustion (25%–42%) and biomass pellet burning (~42%) were comparable but significantly higher than those from raw biomass (22%–31%). The abundance of SOCs was not statistically correlated with the fuel S content in the present study for pooled data. However,

when fuel subgroups were considered, fuels (coal or raw biomass) with a higher sulfur content had higher SOC levels. Also, higher SOC emission was found for pine wood combusted in the improved stove which have higher combustion efficiency than that in the traditional stove. These results suggested that, except for fuel sulfur content, the fuel type and combustion efficiency would also influence the SOC emissions.

In the WIOC, the intensities of these four groups among different rice source samples were different from those in the

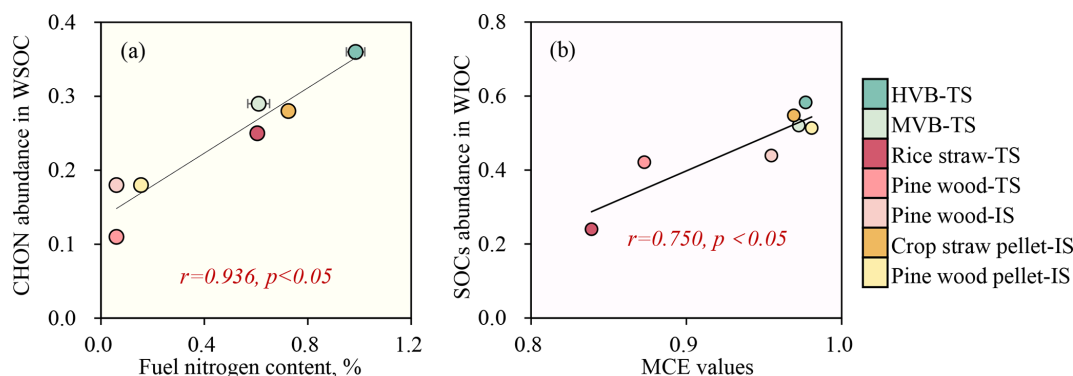


Figure 3. Correlation between fuel nitrogen contents and abundances of CHON in WSOC (a) and the correlation between MCE values and the abundances of SOCs in WIOC (b). TS represents combustion in the traditional stove, and IS represents combustion in the improved stove.

WSOC. The CHO group accounted for 27%–45% raw biomass burning aerosols, 22%–24% biomass pellet smoke, and 13%–22% coal smoke. On the contrary, the SOC abundance was significantly higher in WIOC, especially for the coal, accounting for 58% for HVB and 52% for MVB. A significantly positive correlation between the MCE values and SOC abundance in the WIOC extract was found ($r = 0.750$; $p < 0.05$) (Fig. 3), while no clear association between fuel sulfur content and SOC emissions was observed in the WIOC. Combining the result from the WSOC extract, the strong dependence of SOC emissions on the combustion conditions was expected, while the fuel sulfur content had a slight influence. Notably, the SOC abundance in aerosols from coal combustion was greatly higher than that in ambient aerosols (Lin et al., 2012), indicating that residential non-desulfurized coal combustion might be an important emitter of SOCs in atmospheric samples. The CHON group emissions were determined mainly by the fuel nitrogen content, while SOC emissions were strongly related to the combustion conditions (e.g., flaming phase). It should be noted that the results of our analysis based on the current data without isotopic internal standard used were semi-quantitative, so some uncertainties must be addressed.

3.3 Detailed CHO/CHON/CHOS/CHONS group differences across fuel types

Van Krevelen (VK) diagrams which can provide a visual interpretation of complex mass spectra can qualitatively identify chemical composition profiles in mixtures (Lv et al., 2016). The classification criteria of the VK diagram are provided in Table S3 (Patriarca et al., 2018; Tang et al., 2020). Figures S5 and S6 show the VK diagrams of WSOC and WIOC. In both WSOC and WIOC extracts, the carboxylic-rich alicyclic molecules (CRAM-like) were the most abundant component, contributing 53%–69% in the WSOC extract and 37%–56% in the WIOC extract, respectively. The condensed aromatics were also an important component in source samples, accounting for 7.3%–13% in the WSOC

and for a higher proportion of 8.6%–44% in the WIOC. This observation could be attributed to the hydrophobic property of condensed aromatic hydrocarbons, leading to a lower proportion in the highly polar WSOC. Among the identified formulas, 7.0%–13% of the total intensity in the WSOC and 3.6%–17% in the WIOC were the aliphatic/peptide-like compounds. Such fractions were comparable to unsaturated hydrocarbons with percentages of 3.9%–15% in the WSOC and 2.0%–11% in the WIOC. The compounds including lipid-like species and highly oxygenated compounds (HOCs) were in a relatively lower abundance, with less than 10% each in the source samples. The different fuels showed varied chemical composition characteristics. Coal combustion aerosols had lower H/C ratios than those in biomass burning aerosols, indicating higher unsaturated degrees (Table S2). As indicated by the VK diagrams, the coal combustion produced a notable number of condensed aromatics, contributing to 27%–44% of the WIOC, which was significantly higher than 8.6%–21% in biomass burning emissions. The modified aromaticity index ($AI_{\text{mod,w}}$) which is a measure of aromatic and condensed aromatic structure fractions, and the double-bond equivalent (DBE) values which are used as a measure of the unsaturated level in a molecule were all higher for coal emissions compared to the biomass emissions.

Distinct compound profiles being identified by the VK diagram classification criteria are consistent with discrepancies in the four groups (CHO/CHON/CHOS/CHONS). For the CHO group, the most intense compounds were CRAMs compounds with fractions of 69%–84% in the WSOC extract and higher fractions of 51%–80% in the WIOC extract. It was observed that raw biomass would emit slightly more CRAMs (76%–84% in the WSOC and 61%–80% in the WIOC) than coal (69%–73% in the WSOC and 62%–69% in the WIOC) and biomass pellet (70%–75% in the WSOC and 51%–56% in the WIOC) combustion. The condensed aromatic compound was also a crucial component, accounting for 13%–20% of the WSOC and 19%–27% of

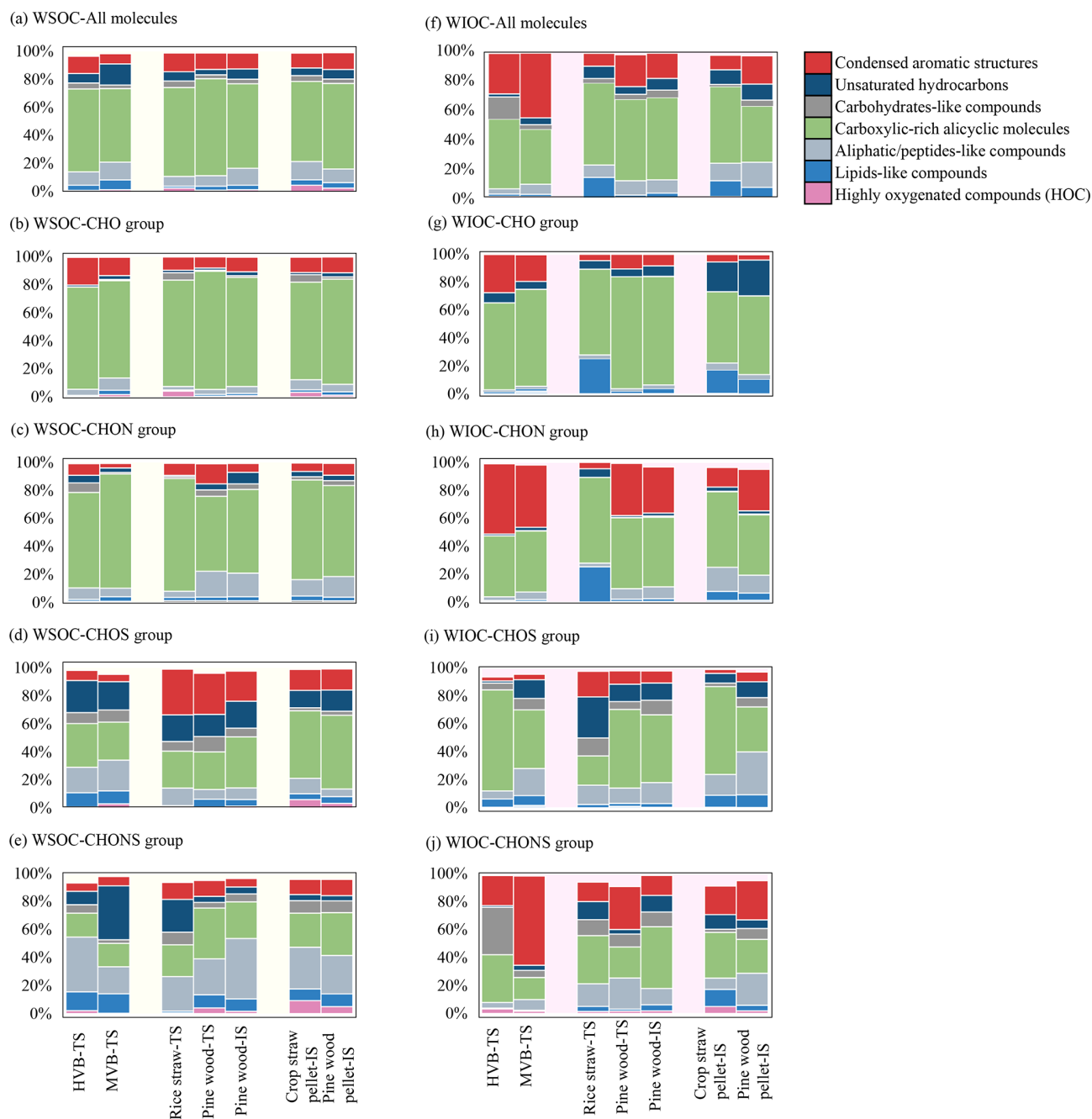


Figure 4. Each component abundance identified by VK diagram of WSOC (**a** – all molecules; **b** – CHO group; **c** – CHON group; **d** – CHOS group; **e** – CHONS group) and WIOC (**f** – all molecules; **g** – CHO group; **h** – CHON group; **i** – CHOS group; **j** – CHONS group). The classification criteria are provided in Table S3.

the WIOC from coal emissions. These fractions were significantly higher than those found in raw biomass (4.5%–10% in the WSOC and 7.9%–10% in the WIOC) and biomass pellets (3.8%–5.4% in the WSOC and 11% in the WIOC) (Fig. 4). The other components accounted for a small contribution (less than 10% each) to the total CHO intensity.

It was reported that the CHON compounds with $O/N \geq 3$ might be the organonitrate candidate and nitro-substituted

compounds attributing to the allocation of one nitro (NO_2) or nitrooxy (ONO_2) group (Bianco et al., 2018). In this study, the relative content of $\text{CHON}_{O/N \geq 3}$ compounds (concerning the overall CHON) in the biomass (raw and pellet ones) ranged between 71%–82% and 85%–91% for the WSOC and WIOC, which is distinctly lower than those found in coal smoke (86%–90% for the WSOC and 86%–95% for the WIOC) (Table S4). Moreover, the $\text{AI}_{\text{mod},w}$ values for

CHON compounds from coal combustion were higher than the biomass smoke for both WSOC and WIOC, as indicated in Table S2. It can thus be concluded that more CHON compounds with low aromaticity and a large number of oxidized nitrogen functional groups were formed during the combustion of biomass fuels. Coal combustion emissions had more intense condensed aromatic compounds with a percentage of 45%–50% for the CHON group, which were significantly higher than those from raw biomass (4.5%–37%) and biomass pellet burning (14%–30%). This result confirmed the conclusion that the CHON compounds produced from the combustion of coal were characterized by a relatively high aromaticity and a low degree of oxidation.

The O-rich CHOS fraction ($O/S \geq 4$) accounted for 42%–71% (concerning the overall CHON group) in the WSOC and 45%–95% in the WIOC. O-rich CHOS fraction ($O/S \geq 4$) content from coal (66%–70% in the WSOC and 78%–98% in the WIOC) and biomass pellet (67%–71% in the WSOC and 76%–87% in the WIOC) was relatively higher than the raw biomass smoke (42%–56% in the WSOC and 32%–57% in the WIOC), suggesting that most of the CHOS compounds in coal and pellet smoke can be potentially assigned with more structures containing the sulfate ($-\text{OSO}_3\text{H}$) or sulfonate ($-\text{SO}_3$) functional groups. Different from CHO and CHON groups, it was found that the CHOS group in the biomass burning aerosols had a much more intense condensed aromatic structure with a percentage of 14%–33% in the WSOC and 2.5%–19% in the WIOC, especially for raw biomass (WSOC 22%–33%; WIOC 8.5%–19%) than coal combustion (WSOC 4.9%–7.0%; WIOC 2.5%–7.0%). For the CHOS group in the WIOC extract, the unsaturated hydrocarbons were also an important component, accounting for 12%–29% of raw biomass burning emissions, which were significantly higher than those in biomass pellets (6.9%–11%) and coal (1.5%–13%). These results indicated biomass burning emissions were characterized by higher unsaturation levels and aromaticity for the CHOS group than coal combustion.

Nearly 34%–85% of CHONS formulas have many O atoms (≥ 7), indicating the existence of the $-\text{NO}_3$ group (Table S4). These CHONS compounds are probably nitroxy-organosulfates (Song et al., 2019). The remaining compounds (15%–66%) of the CHONS group had fewer than seven atoms, implying that large numbers of CHONS compounds were assigned with reduced N (e.g., amide and nitrile and heterocyclic aromatics). The condensed aromatic compounds identified by the VK diagram in the WIOC from coal combustion accounted for 22%–64%, which was relatively higher than those from biomass burning (14%–31%), indicating a higher degree of aromaticity. This was consistent with the difference observed in the $\text{AI}_{\text{mod,w}}$ values as seen in Table S2. The $\text{AI}_{\text{mod,w}}$ of WIOC in coal emissions were 0.38 for HVB and 0.60 for MVB, and the values were higher than the raw biomass (0.32–0.38) and biomass pellets

(0.35–0.36), confirming a higher aromatic compound content of the coal smoke sample than biomass for CHONS group.

Therefore, the CHO, CHON, and CHONS groups generated from coal combustion were characterized by high unsaturated levels with more aromatic species, while CHOS groups had higher aromaticity degrees in biomass smoke aerosols. Aromatic compounds might be the strong BrC chromophores contributing to light absorption (Song et al., 2019). The difference in MAE between coal and biomass emissions and its association with the chemical components will be discussed in detail in Sect. 3.5.

3.4 Likely unique molecules of biomass and coal combustion

The unique molecules may be inferred from the Venn diagram of formulas, as shown in Fig. S7. Among the observed compounds, 3039 and 1624 unique molecular formulas were detected in the combustion of rice straw and pine wood in the traditional stove in the WSOC fractions, which was significantly higher than those found in biomass pellets used in improve stoves (638–696) and coal used in traditional stoves (570–734). This suggested a notable difference between the emissions from raw biomass and coal, even when using the same stove. Interestingly, fewer unique peaks were observed for pine wood used in improved stoves (533), indicating that using an improved stove for raw biomass could narrow the difference between coal and biomass emissions. A similar trend was also found in the WIOC fractions (Fig. S7). The CHONS group accounted for a significant portion of unique formulas in source samples, particularly in coal smoke, representing 51%–52% in the WSOC extract and 51%–69% in the WIOC extract. The important role of the CHONS group in unique emissions from coal combustion was also noted by Tang et al. (2020), who reported that CHO and CHON were the main components of unique molecular formulas of raw biomass burning emissions among the raw biomass burning, coal combustion, and vehicle emissions, representing 88%–93%. This fraction was higher than our result of 33%–77% in raw biomass and only 26%–27% in biomass pellets. The distribution of the unique molecules further indicated substantial discrepancies among the fuels. Unique molecules in coal-combustion-derived aerosols were in the region with lower H/C and O/C values compared with all other samples (Fig. 5) in both WSOC and the WIOC extracts, indicating a higher degree of unsaturation and lower level of oxidation. For example, it was observed that specific emissions from coal combustion were mainly composed of condensed aromatics (32%–59%), followed by CRAMs compounds (23%–39%) in the WIOC extract. However, only 4.3%–9.7% condensed aromatics of the total unique emissions were observed for biomass burning, with CRAMs being the main component (39%–65%). As for different groups of CHO/CHON/CHONS, the condensed aromatic compound contents for all three groups in coal smoke

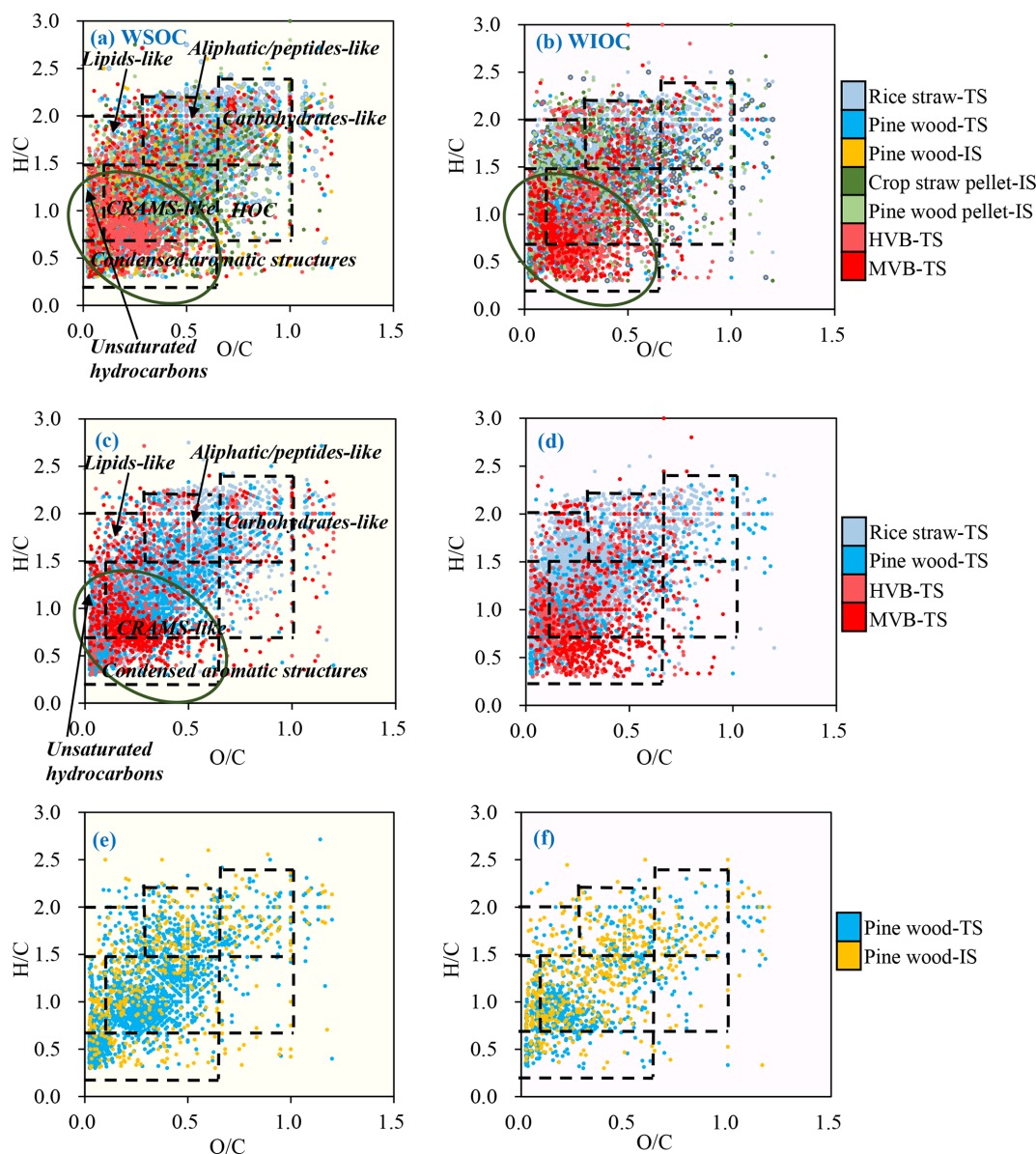


Figure 5. Van Krevelen diagrams of WSOC (a, c, e) and WIOC (b, d, f) from the source samples. TS represents combustion in the traditional stove, and IS represents combustion in the improved stove. Different colors indicate unique formulas detected in each sample of solid fuel combustion.

aerosol (unique detected ones) were relatively higher compared to biomass. While the CHOS group showed a different trend in that condensed the aromatic compound contents of biomass smoke (unique detected ones) were relatively higher than coal smoke in the WSOC extract and comparable to coal smoke in the WIOC extract. This finding highlighted the CHOS group's importance in distinguishing the aerosols from the combustion of coal or biomass, helping conduct the source apportionment of aerosols. Additionally, compared with the pine wood emissions from improved stoves, most unique molecules in aerosol from pine wood combustion in traditional stoves were in the region with lower H/C and O/C

ratios (Fig. 5), which were identified mainly as CRAMs compounds. The emissions from the improved stove were distributed in a wider range with fewer CRAMs compounds and more aliphatic/peptide-like compounds were observed. Unique molecules from biomass pellets combusted in the improved stove distributed in the upper region of the VK diagram with higher H/C values in WIOC extract, which indicated a lower unsaturated degree (Fig. S8).

A total of 484 molecular formulas were detected simultaneously in the seven aerosol samples in the WSOC extract and 306 in the WIOC extract. Among these commonly detected molecules, most of which were CHO compounds,

with the molecular numbers accounting for 60 % and 73 % in the WSOC and WIOC, respectively. CHON accounted for 31 % of WSOC and 19 % of WIOC, while SOCs only occupied about 10 %. As seen in Fig. S9, these CHO compounds were mainly composed of CRAM-like compounds and several lipid-like and aliphatic/peptide-like compounds. Moreover, these compounds were relatively small molecular compounds assigned with 8–28 C atoms and 2–12 O atoms, with DBE values of 2–17 for the WSOC extract. The relatively more C atoms assigned with larger DBE values were observed for the CHO compounds in WIOC, which could be partially explained by the fact that the overall CHO compounds in the WIOC extract had larger MW values with a high degree of unsaturation. In total, the CHON compounds were also CRAM-like compounds, and almost no compounds were expected to be aromatics. CHOS and CHONS species had much fewer formulas, especially for CHONS, that only accounted for 1.0 % of the commonly detected molecules in the WIOC. The unsaturated levels of commonly detected molecules in all seven source samples were relatively low. For example, the condensed aromatic compounds accounted for 6.5 %–9.3 % and 3.3 %–4.1 % of the total intensity for coal smoke and biomass smoke in the WSOC, respectively, as well as 0.38 %–8.3 % and 18 %–21 % in the WIOC extract. Different from the CHO, CHON, and CHONS groups, high percentages of condensed aromatic compounds were found in the CHOS group (commonly detected ones) from raw biomass burning aerosols, with a range of 6.6 %–51 % in the WSOC extract and 12 %–46 % in the WIOC extract. These fractions were significantly higher than those from coal smoke (4.1 %–4.9 % in the WSOC extract and 8.8 %–25 % in the WIOC extract). This combined the finding that the CHOS group in biomass smoke had a higher-aromaticity degree in both WSOC and WIOC extracts. However, the unique molecules in the WIOC extract did not follow this trend. It was thus speculated that the higher-aromaticity degree of the CHOS group in biomass smoke was attributed to the intensity variation in these simultaneously detected compounds rather than the unique emission from a special source for the WIOC extract.

To explore the potential influence of fuel properties and combustion conditions on chemical composition, the major factors such as fuel moisture, V_{daf} , and parameters reflecting combustion conditions, including MCE and EC/OC ratios, were assessed. The linear correlation analysis was applied to estimate the effect of these factors on each molecular intensity (commonly detected ones) (Figs. S10 and S11). The aliphatic compounds (including lipid-like, aliphatic/peptide-like, and carbohydrate-like compounds) were negatively correlated with the fuel moisture and positively correlated with V_{daf} and EC/OC ratios. Fuel moisture has been recognized as an important factor influencing pollutant formation, but the influence is usually very complicated. The observed relationship between fuel water content and pollutant EFs varies largely among studies, which may be attributed to factors

such as different water contents, pollutant types, and interactions among other influencing factors. Fuels with high moisture levels may have high emissions as extra energy is needed to vaporize water during the burning process; however, a decrease in combustion temperatures under very high water content conditions may slow the pollutant formation rate and consequently lower emissions. Higher EC/OC ratios and larger MCE values tend to be associated with stronger flaming conditions. The results suggested that the aliphatic compounds were apt to be produced during the period of the flaming phase with higher combustion temperature. This result could partially explain that aliphatic/peptide-like compounds would be apt to be produced in the improved stove rather than the traditional stove. In comparison, the emissions of CRAM-like compounds, which are the most abundant species, were decreased with the increased MCE and EC/OC values, indicating that CRAM-like compounds were generated under the smoking phase. No significant correlations of aromatics, unsaturated hydrocarbons, and HOCs were observed with these parameters, resultant from their small proportion in commonly detected molecules. It is worth noting that there may be significant differences, even for the same fuel, in chemical composition that depend on other factors such as stove type and combustion conditions. The interactions among these factors make it difficult to assess their influence. It was found that only around 50 % of the identified molecules were overlapped emissions for pine wood combusted in the traditional stove and in the improved stove, suggesting the importance of the stove used. A smaller fraction of 25 %–30 % of molecules was observed compared to the pine wood emissions with coal combusted in the same stove, which suggested that the influence of varied fuels on chemical composition could surpass the differences caused by different stoves. Our previous studies have revealed that the fuel type was the most important factor influencing the MAE values (Zhang et al., 2021b) and BrC EFs (Zhang et al., 2021a). The present study highlighted the dominant effect of fuel type on the chemical composition of soluble OC, providing a theoretical basis for source appointment based on molecular composition. Moreover, the combustion conditions would have a significant effect on the molecular intensity, resulting in differences in MAE eventually, as indicated in Sect. 3.1.

3.5 The correlation of light absorption properties with molecular compositions

Here we specifically investigate the variability in optical characteristics among the different fuels attributed to their chemical compositions. No significant correlations were observed between the AAE values of soluble OC and the molecular composition, indicating that AAE could be influenced by many factors. The MAE may be influenced by the degree of oxidation and unsaturation degree (Mo et al., 2017) (Tang et al., 2020); however, there was no significant correlation found between the MAE values and O/C values in the

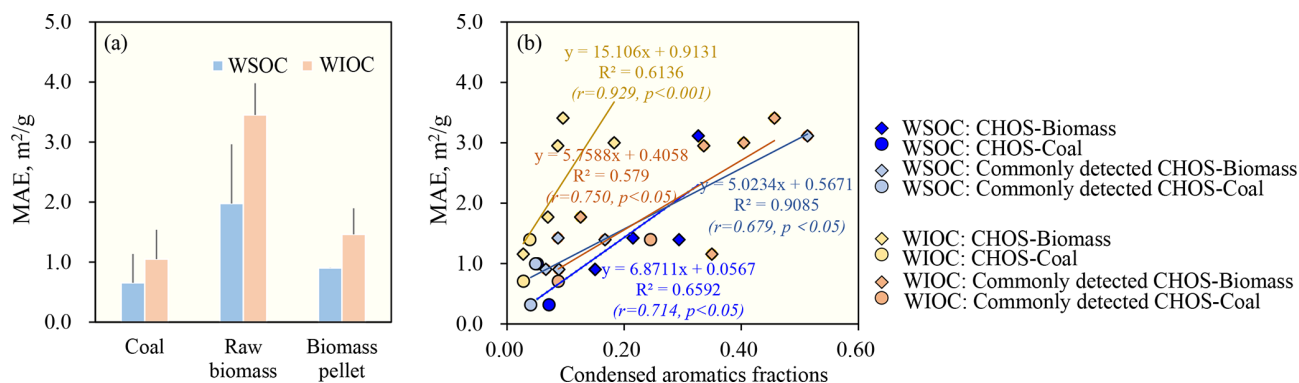


Figure 6. MAE values at λ 365 nm (a) and correlations between MAE values and condensed aromatic fractions in CHOS and in commonly detected CHOS (b) from the source samples.

present source samples, implying that the BrC light absorption ability might not be directly affected by its oxidation degree.

The $MAE_{365, WSOC}$ values were significantly positively correlated with the DBE values ($r = 0.786$; $p < 0.05$) and the MW values ($r = 0.750$; $p < 0.05$) (Fig. S12), indicating that unsaturation and MW played a crucial role in the light absorption capability of the source samples. In the above discussion, we have noticed that the CHOS group in biomass was characterized by a higher degree of aromaticity than coal smoke aerosol, while the CHO, CHON, and CHONS groups have a higher-aromaticity degree in the coal emissions. A significantly positive correlation ($r = 0.714$; $p < 0.05$) was observed between $MAE_{365, WSOC}$ values and the condensed aromatics percentages from the CHOS group (Fig. 6), indicating that aromatics in the CHOS group contributed to the high light absorption ability of biomass smoke.

For the WIOC extract, no significant correlation was found between the $MAE_{365, WIOC}$ values with MW or DBE values, which might be explained by the very different chemical composition for insoluble compounds compared with soluble parts. Although the coal combustion emitted much more aromatic compounds with higher DBE values for the WIOC, the MAE values were not significantly higher. The significantly positive correlation ($r = 0.929$; $p < 0.05$) between $MAE_{365, WIOC}$ values and the CHOS condensed aromatics percentages confirmed the importance of CHOS aromatics in determining the light absorption capability from source samples. As mentioned in Sect. 3.4, the higher-aromaticity degree of the CHOS group in biomass smoke was largely due to the intensity variation in these commonly detected compounds in all source samples. Further analysis revealed that $MAE_{365, WIOC}$ values were positively correlated ($r = 0.750$; $p < 0.05$) with the CHOS condensed aromatic fractions which were the fraction simultaneously detected in all samples. These results indicated that the light absorption capability of source aerosols may be due to the higher abun-

dance of some CHOS aromatic compounds commonly emitted from both coal and biomass rather than the unique tracers.

4 Conclusion and implication

The $MAE_{365, WSOC}$ ranged from 0.21 to 3.1 m² g⁻¹, with an average of 1.3 ± 0.7 m² g⁻¹. The $MAE_{365, WIOC}$ was found to be higher, with an average of 2.0 ± 1.3 m² g⁻¹. There were significant differences ($p < 0.05$) observed among the different fuels for both $MAE_{365, WSOC}$ and $MAE_{365, WIOC}$ as raw biomass burning combustion had significantly higher values than the coal combustion. The AAE_{WSOC} ranged from 3.8 to 11, with an average of 6.9 ± 1.5 . The AAE_{WIOC} was slightly lower than AAE_{WSOC} , which ranged from 4.2 to 6.5 with an average of 5.5 ± 0.5 . Thousands of peaks were identified in the m/z range of 150–800, indicating a complex chemical composition of aerosols from residential sources. The CHO group was the most abundant component in the WSOC extract, and the contribution of CHO compounds to the total intensity in aerosols from raw biomass burning was significantly higher than those from biomass pellets and coal smoke. On the other hand, the WIOC extract contained more SOCs, especially in the coal combustion aerosol. Notably, CHON compounds were more abundant in the coal combustion emissions, which was due to the higher fuel N content of coal ($r = 0.936$; $p < 0.05$). The SOC emissions were more predominant during flaming phases, with a positive correlation between SOC abundance with the MCE values ($r = 0.750$; $p < 0.05$). The CHO, CHON, and CHONS groups generated from coal combustion were characterized by high unsaturated levels with more aromatic species, while CHOS groups had higher-aromaticity degrees in biomass smoke aerosols. It was found that MAE values were positively correlated with the CHOS condensed aromatic proportion for both the WSOC ($r = 0.714$; $p < 0.05$) and WIOC extracts ($r = 0.929$; $p < 0.001$). These results indicated that higher CHOS-condensed aromatic abundance in biomass burning aerosols could partly explain the higher MAE val-

ues of the raw biomass smoke. Further analysis showed a positive correlation of MAE with the CHOS-condensed aromatic fractions, which were the fractions simultaneously detected in all samples. These results indicated that the light absorption capability of source aerosols may be due to the higher abundance of some CHOS aromatic compounds commonly emitted from both coal and biomass burning rather than the unique tracers. The unique formulas of coal combustion aerosols were in the lower H/C and O/C regions, with higher unsaturated compounds in the VK diagram. This work is potentially applicable to the source appointment, based on the molecular characteristics, and to future studies developing more scientific control measures by focusing on one major component (e.g., CHOS condensed aromatics) of light absorption aerosols.

There are still some questions that need to be investigated in a future study. First, the study on BrC composition in this research used dissolved OC as a substitute. However, this substitute cannot fully represent BrC emissions. Both WSOC and WIOC contain some non-light-absorbing components, and the proportion of these components is unknown, making it difficult to measure the representativeness of extractable OC for BrC. Additionally, a lack of research about the emission characteristics under controlled combustion conditions limits the obtained results. Controlled experiments including flaming or smoldering burns, airflow, and combustion temperature are needed in future work. Third, fresh burning-derived OC released into the atmosphere can undergo various aging reactions such as photochemical degradation. These reactions can significantly alter the light absorptivity and chemical properties of BrC components. It is essential to consider the optical properties and lifetimes of organic compounds emitted from solid fuel combustion in climate models.

Data availability. Data are available by contacting the corresponding authors.

Supplement. The following information is in the Supplement: data processing in the ESI FT-ICR-MS; fuel properties of the coal and biomass fuels tested; the number of formulas in each group, values of elemental ratios, MW, and DBE values in the WSOC and WIOC for each source type; stoichiometric ranges of VK classes; the correlation between fuel N and emission factors of NO_x ; the VK diagrams of WSOC and WIOC for different source samples; and correlations between the VK plots of WSOC/WIOC and fuel properties or combustion conditions. The supplement related to this article is available online at: <https://doi.org/10.5194/acp-24-6323-2024-supplement>.

Author contributions. LZ, GS, and ST designed the experiment. LZ and JL prepared the filters used. LZ, YL, XL, and ZL conducted

the sample collection. LZ and JL performed the data analysis. LZ wrote the paper. GS and ST reviewed and commented on the paper.

Competing interests. The contact author has declared that none of the authors has any competing interests.

Disclaimer. Publisher's note: Copernicus Publications remains neutral with regard to jurisdictional claims made in the text, published maps, institutional affiliations, or any other geographical representation in this paper. While Copernicus Publications makes every effort to include appropriate place names, the final responsibility lies with the authors.

Acknowledgements. The authors greatly appreciated the valuable help in data analysis by Jianzhong Song from the Chinese Academy of Sciences (CAS).

Financial support. Funding for this study was partly from the National Natural Science Foundation of China (grant nos. 42077328 and 41922057).

Review statement. This paper was edited by Dantong Liu and reviewed by two anonymous referees.

References

- Bianco, A., Deguillaume, L., Vaitilingom, M., Nicol, E., Baray, J. L., Chaumerliac, N., and Bridoux, M.: Molecular Characterization of Cloud Water Samples Collected at the Puy de Dome (France) by Fourier Transform Ion Cyclotron Resonance Mass Spectrometry, *Environ. Sci. Technol.*, 52, 10275–10285, <https://doi.org/10.1021/acs.est.8b01964>, 2018.
- Bond, T. C.: Spectral dependence of visible light absorption by carbonaceous particles emitted from coal combustion, *Geophys. Res. Lett.*, 28, 4075–4078, <https://doi.org/10.1029/2001GL013652>, 2001.
- Bond, T. C. and Bergstrom, R. W.: Light absorption by carbonaceous particles: An investigative review, *Aerosol Sci. Tech.*, 40, 27–67, <https://doi.org/10.1080/02786820500421521>, 2006.
- Cao, T., Li, M., Zou, C., Fan, X., Song, J., Jia, W., Yu, C., Yu, Z., and Peng, P.: Chemical composition, optical properties, and oxidative potential of water- and methanol-soluble organic compounds emitted from the combustion of biomass materials and coal, *Atmos. Chem. Phys.*, 21, 13187–13205, <https://doi.org/10.5194/acp-21-13187-2021>, 2021.
- Chen, Y. and Bond, T. C.: Light absorption by organic carbon from wood combustion, *Atmos. Chem. Phys.*, 10, 1773–1787, <https://doi.org/10.5194/acp-10-1773-2010>, 2010.
- Du, Z., He, K., Cheng, Y., Duan, F., Ma, Y., Liu, J., Zhang, X., Zheng, M., and Weber, R.: A yearlong study of water-soluble organic carbon in Beijing II: Light absorption properties, *Atmos. Environ.*, 89, 235–241, <https://doi.org/10.1016/j.atmosenv.2014.02.022>, 2014.

- Feng, Y., Ramanathan, V., and Kotamarthi, V. R.: Brown carbon: a significant atmospheric absorber of solar radiation?, *Atmos. Chem. Phys.*, 13, 8607–8621, <https://doi.org/10.5194/acp-13-8607-2013>, 2013.
- Guan, D., Shen, Z., and Chen, Q.: Formation and elimination of brown carbon aerosol: A review, *Environ. Chem.*, 39, 2812–2822, <https://doi.org/10.7524/j.issn.0254-6108.2022051801>, 2020.
- Hansson, K. M., Samuelsson, J., Tullin, C., and Amand, L. E.: Formation of HNCO, HCN, and NH₃ from the pyrolysis of bark and nitrogen-containing model compounds, *Combust. Flame*, 137, 265–277, <https://doi.org/10.1016/j.combustflame.2004.01.005>, 2004.
- He, T., Wu, Y., Wang, D., Cai, J., Song, J., Yu, Z., Zeng, X., and Peng, P. a.: Molecular compositions and optical properties of water-soluble brown carbon during the autumn and winter in Guangzhou, China, *Atmos. Environ.*, 296, 119573, <https://doi.org/10.1016/j.atmosenv.2022.119573>, 2023.
- Holder, A. L., Hagler, G. S. W., Aurell, J., Hays, M. D., and Gullett, B. K.: Particulate matter and black carbon optical properties and emission factors from prescribed fires in the southeastern United States, *J. Geophys. Res.-Atmos.*, 121, 3465–3483, <https://doi.org/10.1002/2015JD024321>, 2016.
- Huang, R. J., Yang, L., Cao, J., Chen, Y., Chen, Q., Li, Y., Duan, J., Zhu, C., Dai, W., Wang, K., Lin, C., Ni, H., Corbin, J. C., Wu, Y., Zhang, R., Tie, X., Hoffmann, T., O'Dowd, C., and Dusek, U.: Brown Carbon Aerosol in Urban Xi'an, Northwest China: The Composition and Light Absorption Properties, *Environ. Sci. Technol.*, 52, 6825–6833, <https://doi.org/10.1021/acs.est.8b02386>, 2018.
- Huang, R. J., Yang, L., Shen, J., Yuan, W., Gong, Y., Guo, J., Cao, W., Duan, J., Ni, H., Zhu, C., Dai, W., Li, Y., Chen, Y., Chen, Q., Wu, Y., Zhang, R., Dusek, U., O'Dowd, C., and Hoffmann, T.: Water-Insoluble Organics Dominate Brown Carbon in Wintertime Urban Aerosol of China: Chemical Characteristics and Optical Properties, *Environ. Sci. Technol.*, 54, 7836–7847, <https://doi.org/10.1021/acs.est.0c01149>, 2020.
- Huo, Y., Li, M., Jiang, M., and Qi, W.: Light absorption properties of HULIS in primary particulate matter produced by crop straw combustion under different moisture contents and stacking modes, *Atmos. Environ.*, 191, 490–499, <https://doi.org/10.1016/j.atmosenv.2018.08.038>, 2018.
- Jiang, H., Li, J., Sun, R., Tian, C., Tang, J., Jiang, B., Liao, Y., Chen, C.-E., and Zhang, G.: Molecular Dynamics and Light Absorption Properties of Atmospheric Dissolved Organic Matter, *Environ. Sci. Technol.*, 55, 10268–10279, <https://doi.org/10.1021/acs.est.1c01770>, 2021.
- Jo, D. S., Park, R. J., Lee, S., Kim, S.-W., and Zhang, X.: A global simulation of brown carbon: implications for photochemistry and direct radiative effect, *Atmos. Chem. Phys.*, 16, 3413–3432, <https://doi.org/10.5194/acp-16-3413-2016>, 2016.
- Laskin, A., Laskin, J., and Nizkorodov, S. A.: Chemistry of Atmospheric Brown Carbon, *Chem. Rev.*, 115, 4335–4382, <https://doi.org/10.1021/cr5006167>, 2015.
- Li, J., Zhang, Q., Wang, G., Li, J., Wu, C., Liu, L., Wang, J., Jiang, W., Li, L., Ho, K. F., and Cao, J.: Optical properties and molecular compositions of water-soluble and water-insoluble brown carbon (BrC) aerosols in northwest China, *Atmos. Chem. Phys.*, 20, 4889–4904, <https://doi.org/10.5194/acp-20-4889-2020>, 2020.
- Li, M., Fan, X., Zhu, M., Zou, C., Song, J., Wei, S., Jia, W., and Peng, P. A.: Abundance and Light Absorption Properties of Brown Carbon Emitted from Residential Coal Combustion in China, *Environ. Sci. Technol.*, 53, 595–603, <https://doi.org/10.1021/acs.est.8b05630>, 2019.
- Lin, P., Rincon, A. G., Kalberer, M., and Yu, J. Z.: Elemental Composition of HULIS in the Pearl River Delta Region, China: Results Inferred from Positive and Negative Electrospray High Resolution Mass Spectrometric Data, *Environ. Sci. Technol.*, 46, 7454–7462, <https://doi.org/10.1021/es300285d>, 2012.
- Lv, J., Zhang, S., Wang, S., Luo, L., Cao, D., and Christie, P.: Molecular-Scale Investigation with ESI-FT-ICR-MS on Fractionation of Dissolved Organic Matter Induced by Adsorption on Iron Oxyhydroxides, *Environ. Sci. Technol.*, 50, 2328–2336, <https://doi.org/10.1021/acs.est.5b04996>, 2016.
- Mo, Y., Li, J., Liu, J., Zhong, G., Cheng, Z., Tian, C., Chen, Y., and Zhang, G.: The influence of solvent and pH on determination of the light absorption properties of water-soluble brown carbon, *Atmos. Environ.*, 161, 90–98, <https://doi.org/10.1016/j.atmosenv.2017.04.037>, 2017.
- Mo, Y., Zhong, G., Li, J., Liu, X., Jiang, H., Tang, J., Jiang, B., Liao, Y., Cheng, Z., and Zhang, G.: The Sources, Molecular Compositions, and Light Absorption Properties of Water-Soluble Organic Carbon in Marine Aerosols From South China Sea to the Eastern Indian Ocean, *J. Geophys. Res.-Atmos.*, 127, e2021JD036168, <https://doi.org/10.1029/2021JD036168>, 2022.
- Olson, M. R., Garcia, M. V., Robinson, M. A., Van Rooy, P., Diitenberger, M. A., Bergin, M., and Schauer, J. J.: Investigation of black and brown carbon multiple-wavelength-dependent light absorption from biomass and fossil fuel combustion source emissions, *J. Geophys. Res.-Atmos.*, 120, 6682–6697, <https://doi.org/10.1002/2014JD022970>, 2015.
- Park, S. S. and Yu, J.: Chemical and light absorption properties of humic-like substances from biomass burning emissions under controlled combustion experiments, *Atmos. Environ.*, 136, 114–122, <https://doi.org/10.1016/j.atmosenv.2016.04.022>, 2016.
- Patriarca, C., Bergquist, J., Sjoberg, P. J. R., Tranvik, L., and Hawkes, J. A.: Online HPLC-ESI-HRMS Method for the Analysis and Comparison of Different Dissolved Organic Matter Samples, *Environ. Sci. Technol.*, 52, 2091–2099, <https://doi.org/10.1021/acs.est.7b04508>, 2018.
- Pokhrel, R. P., Wagner, N. L., Langridge, J. M., Lack, D. A., Jayarathne, T., Stone, E. A., Stockwell, C. E., Yokelson, R. J., and Murphy, S. M.: Parameterization of single-scattering albedo (SSA) and absorption Ångström exponent (AAE) with EC/OC for aerosol emissions from biomass burning, *Atmos. Chem. Phys.*, 16, 9549–9561, <https://doi.org/10.5194/acp-16-9549-2016>, 2016.
- Rathod, T., Sahu, S. K., Tiwari, M., Yousaf, A., Bhangare, R. C., and Pandit, G. G.: Light Absorbing Properties of Brown Carbon Generated from Pyrolytic Combustion of Household Biofuels, *Aerosol Air Qual. Res.*, 17, 108–116, <https://doi.org/10.4209/aaqr.2015.11.0639>, 2017.
- Saleh, R., Robinson, E. S., Tkacik, D. S., Ahern, A. T., Liu, S., Aiken, A. C., Sullivan, R. C., Presto, A. A., Dubey, M. K., Yokelson, R. J., Donahue, N. M., and Robinson, A. L.: Brownness of organics in aerosols from biomass burning linked to their black carbon content, *Nat. Geosci.*, 7, 647–650, <https://doi.org/10.1038/ngeo2220>, 2014.

- Song, J., Li, M., Jiang, B., Wei, S., Fan, X., and Peng, P. A.: Molecular Characterization of Water-Soluble Humic like Substances in Smoke Particles Emitted from Combustion of Biomass Materials and Coal Using Ultrahigh-Resolution Electrospray Ionization Fourier Transform Ion Cyclotron Resonance Mass Spectrometry, *Environ. Sci. Technol.*, 52, 2575–2585, <https://doi.org/10.1021/acs.est.7b06126>, 2018.
- Song, J., Li, M., Fan, X., Zou, C., Zhu, M., Jiang, B., Yu, Z., Jia, W., Liao, Y., and Peng, P. a.: Molecular Characterization of Water- and Methanol-Soluble Organic Compounds Emitted from Residential Coal Combustion Using Ultrahigh-Resolution Electrospray Ionization Fourier Transform Ion Cyclotron Resonance Mass Spectrometry, *Environ. Sci. Technol.*, 53, 13607–13617, <https://doi.org/10.1021/acs.est.9b04331>, 2019.
- Sun, J., Zhi, G., Hitznerberger, R., Chen, Y., Tian, C., Zhang, Y., Feng, Y., Cheng, M., Zhang, Y., Cai, J., Chen, F., Qiu, Y., Jiang, Z., Li, J., Zhang, G., and Mo, Y.: Emission factors and light absorption properties of brown carbon from household coal combustion in China, *Atmos. Chem. Phys.*, 17, 4769–4780, <https://doi.org/10.5194/acp-17-4769-2017>, 2017.
- Tang, J., Li, J., Su, T., Han, Y., Mo, Y., Jiang, H., Cui, M., Jiang, B., Chen, Y., Tang, J., Song, J., Peng, P., and Zhang, G.: Molecular compositions and optical properties of dissolved brown carbon in biomass burning, coal combustion, and vehicle emission aerosols illuminated by excitation–emission matrix spectroscopy and Fourier transform ion cyclotron resonance mass spectrometry analysis, *Atmos. Chem. Phys.*, 20, 2513–2532, <https://doi.org/10.5194/acp-20-2513-2020>, 2020.
- Wang, Q. Q., Zhou, Y. Y., Ma, N., Zhu, Y., Zhao, X. C., Zhu, S. W., Tao, J. C., Hong, J., Wu, W. J., Cheng, Y. F., and Su, H.: Review of Brown Carbon Aerosols in China: Pollution Level, Optical Properties, and Emissions, *J. Geophys. Res.-Atmos.*, 127, e2021JD035473, <https://doi.org/10.1029/2021JD035473>, 2022.
- Wozniak, A. S., Bauer, J. E., Sleighter, R. L., Dickhut, R. M., and Hatcher, P. G.: Technical Note: Molecular characterization of aerosol-derived water soluble organic carbon using ultrahigh resolution electrospray ionization Fourier transform ion cyclotron resonance mass spectrometry, *Atmos. Chem. Phys.*, 8, 5099–5111, <https://doi.org/10.5194/acp-8-5099-2008>, 2008.
- Xie, M. J., Hays, M. D., and Holder, A. L.: Light-absorbing organic carbon from prescribed and laboratory biomass burning and gasoline vehicle emissions, *Sci. Rep.-UK*, 7, 7318, <https://doi.org/10.1038/s41598-017-06981-8>, 2017.
- Xiong, R., Li, J., Zhang, Y., Zhang, L., Jiang, K., Zheng, H., Kong, S., Shen, H., Cheng, H., Shen, G., and Tao, S.: Global brown carbon emissions from combustion sources, *Environ. Sci. Ecotechnology*, 12, 100201, <https://doi.org/10.1016/j.ese.2022.100201>, 2022.
- Yokelson, R. J., Susott, R., Ward, D. E., Reardon, J., and Griffith, D. W. T.: Emissions from smoldering combustion of biomass measured by open-path Fourier transform infrared spectroscopy, *J. Geophys. Res.-Atmos.*, 102, 18865–18877, <https://doi.org/10.1029/97jd00852>, 1997.
- Yue, S., Zhu, J., Chen, S., Xie, Q., Li, W., Li, L., Ren, H., Su, S., Li, P., Ma, H., Fan, Y., Cheng, B., Wu, L., Deng, J., Hu, W., Ren, L., Wei, L., Zhao, W., Tian, Y., Pan, X., Sun, Y., Wang, Z., Wu, F., Liu, C.-Q., Su, H., Penner, J. E., Poschl, U., Andreae, M. O., Cheng, Y., and Fu, P.: Brown carbon from biomass burning imposes strong circum-Arctic warming, *One Earth*, 5, 293–304, <https://doi.org/10.1016/j.oneear.2022.02.006>, 2022.
- Zhang, L., Luo, Z., Du, W., Li, G., Shen, G., Cheng, H., and Tao, S.: Light absorption properties and absorption emission factors for indoor biomass burning, *Environ. Pollut.*, 267, 115652, <https://doi.org/10.1016/j.envpol.2020.115652>, 2020.
- Zhang, L., Luo, Z. H., Li, Y. J., Chen, Y. C., Du, W., Li, G., Cheng, H. F., Shen, G. F., and Tao, S.: Optically Measured Black and Particulate Brown Carbon Emission Factors from Real-World Residential Combustion Predominantly Affected by Fuel Differences, *Environ. Sci. Technol.*, 55, 169–178, <https://doi.org/10.1021/acs.est.0c04784>, 2021a.
- Zhang, L., Luo, Z., Xiong, R., Liu, X., Li, Y., Du, W., Chen, Y., Pan, B., Cheng, H., Shen, G., and Tao, S.: Mass Absorption Efficiency of Black Carbon from Residential Solid Fuel Combustion and Its Association with Carbonaceous Fractions, *Environ. Sci. Technol.*, 55, 10662–10671, <https://doi.org/10.1021/acs.est.1c02689>, 2021b.
- Zhang, L., Hu, B., Liu, X., Luo, Z., Xing, R., Li, Y., Xiong, R., Li, G., Cheng, H., Lu, Q., Shen, G., and Tao, S.: Variabilities in Primary N-Containing Aromatic Compound Emissions from Residential Solid Fuel Combustion and Implications for Source Tracers, *Environ. Sci. Technol.*, 13622–13633, <https://doi.org/10.1021/acs.est.2c03000>, 2022.